

OBSERVING ATMOSPHERIC WATER IN STORMS  
WITH THE NIMBUS 7 SCANNING MULTICHANNEL  
MICROWAVE RADIOMETER

Kristina B. Katsaros

Robert M. Lewis

Department of Atmospheric Sciences  
University of Washington  
Seattle, Washington 98195  
U.S.A.ABSTRACT

Employing data on integrated atmospheric water vapor, total cloud liquid water and rain rate obtainable from the Nimbus 7 Scanning Multichannel Microwave Radiometer (SMNR), we study the frontal structure of several mid-latitude cyclones over the North Pacific Ocean as they approach the West Coast of North America in the winter of 1979. The fronts, analyzed with all available independent data, are consistently located at the leading edge of the strongest gradient in integrated water vapor. The cloud liquid water content, which unfortunately has received very little in situ verification, has patterns which are consistent with the structure seen in visible and infrared imagery. The rain distribution is also a good indicator of frontal location and rain amounts are generally within a factor of two of what is observed with rain gauges on the coast. Furthermore, the onset of rain on the coast can often be accurately forecast by simple advection of the SMNR observed rain areas.

## 1. INTRODUCTION

The Scanning Multichannel Microwave Radiometer, SMNR, on Nimbus 7 has been observing brightness temperatures of the Earth and its atmosphere since October 1979, and is still functioning at the time of writing of this report, early 1984. This is quite an engineering accomplishment. A long time series like this is always valuable in geophysical work. Degradation of sensors with time makes interpretation in terms of absolute values difficult, however, and it is wise not to overinterpret. Even though there have been many passive microwave sensors launched over the last decade (Njoku 1982), the SMNR instrument was experimental and there has been considerable difficulty with calibration and correction for the antenna pattern. Gloersen et al. (1984) describe the NASA appointed experiment team's efforts at sorting out these problems, and the work continues. Involved with the engineering type difficulties are the limitations in our ability to assess the accuracy of the geophysical interpretation, because our algorithms are based on very incomplete understanding of the geophysical phenomena per se as well as incomplete understanding of the interaction of microwave radiation with them. These limitations of the present state-of-the-art are the challenge which we must meet vigorously, because as we hope to illustrate with the case studies below, the information obtainable from SMNR - in our case atmospheric water parameters - is tantalizing. It is far more detailed than one might have expected, and provides entirely new kinds of geophysical measurements. History teaches us that the availability of new types of data usually leads to new depths of understanding. Besides the uses one can foresee in research, the SMNR-derived measurements of

atmospheric water parameters also has potential for improving short-range weather forecasting over the sea and in coastal regions.

This study is part of the Nimbus 7 Experiment Team's effort to verify the geophysical parameters produced by the algorithms. In this report we only present data from the first year's record of brightness temperatures which have now been archived. The choice of study area and time frame is based on the availability of high quality in situ data from the CYCLonic Extratropical Storms (CYCLES) Project carried out by the University of Washington Cloud Physics Group under Professor Peter V. Hobbs.

## 2. BACKGROUND ON THE SCANNING MULTICHANNEL MICROWAVE RADIOMETER DATA

For the two case studies reported here we use SMMR data on integrated water vapor, integrated liquid water and rainfall rate. The water vapor emission is measured at 21 GHz near the maximum of the 22 GHz water vapor band, and the Rayleigh and Mie type scattering by cloud and rain drops is observed at 18 and 37 GHz. These emissions can only be discerned against the background of the oceans, which has low brightness temperature due to its low emissivity. Land surfaces emit strongly obscuring cloud and water vapor emissions. Thus, passive microwave sensing of atmospheric water can only be used over the oceans at these frequencies.

### 2.1 Brief Description of the SMMR Instrument

The Scanning Multichannel Microwave Radiometer consists of five concentric antennae, which measure radiances at 6.6, 10.4, 18, 21, and 37 GHz in two polarizations. The Nimbus 7 SMMR scanned 25° to each side of nadir from an altitude of 800 km resulting in ground resolution of 60 km for the 18 and 21 GHz channels and a possible maximum resolution of 30 for the 37 GHz channel. Verification of the interpretation of SMMR-derived atmospheric water parameters has been done to a greater extent for the sister instrument on the Seasat Satellite which operated for three months in 1978 (e.g., Katsaros et al., 1981; Taylor et al., 1983; Alishouse, 1983; McMurdie, 1983). The integrated water vapor has consistently been found to agree both in mean and standard deviation with values obtained by integrating the vapor content measured by radiosonde ascents. The calculated liquid water contents show patterns which agree qualitatively with the cloud distribution on visible or infrared satellite images and the rain rates produced by SMMR algorithms typically agree in a qualitative sense with the subjective coding of rainfall in the synoptic ship reports.

### 2.2 Algorithms

The results presented here are based on the integrated water vapor data archived in the geophysical data record, which has been calculated with an algorithm according to Wilhelm and Chang (1980). However, bias corrections to the brightness temperatures and other corrections have also been applied (see Nimbus 7 SMMR User's Guide, 1984). The cloud liquid water and rainfall rate were calculated with special so-called "team" algorithms from the 18 GHz and 37 GHz horizontal polarization brightness temperatures. Cloud liquid water and rainfall rate are not archived due to the very limited verification and the much greater uncertainty in the underlying physics for these parameters. Emissions at 37 GHz by raindrops are known to depend on the freezing level in the cloud and the drop size distribution, but variations in these quantities are not at present included in any way in the algorithms.

The liquid water algorithm gives "funny numbers," i.e., there are even negative numbers at present, but this is probably only a bias effect, and the

ORIGINAL PAGE IS  
OF POOR QUALITY

patterns obtained by contouring appear reasonable. The rainfall rate algorithm used was the following:

$$RR = (TB_{37H} - 190)/10.0 \quad (1)$$

where RR is the rain rate with units of mm/hr,  $TB_{37H}$  is the brightness temperature in the 37 GHz horizontal polarization channel.

### 3. CASE STUDIES

It is fortunate that early in the Nimbus 7 mission the CYCLES project was operating radars and rain gauges on the west coast of the State of Washington. Information on the rain distribution and amounts from these two sources will be brought to bear on the SMMR observations in case study A below. Because of the fine resolution of the 5.45 cm wavelength radar from the National Center for Atmospheric Research (1° beamwidth, 280 m range gate spacing) and the fine resolution of the tipping bucket rain gauges (typically 0.05 mm), we have the opportunity to look at whether the known mismatch between the resolution of SMMR (at best 30 km) and typical spatial scales of precipitating areas is a serious problem. The rain areas are often oblong, typically 3 to 5 km wide and 18 to 41 km long in these storms (e.g. Persson, 1980).

#### 3.1 Case Study A: Portion of Orbit 1743 Off the Coast of the Pacific Northwest, Centered at 0104 PST, 27 February 1979

The SMMR swath for this study intersected a well defined cold front as it was crossing the coastline of the State of Washington. It is seen in the surface weather map for 0100 PST (Fig. 1) and the GOES-West IR imagery at 0045 PST (Fig. 2). The SMMR map of integrated water vapor is found in Fig. 3. The frontal location shown has been found independently of the SMMR data by careful examination of the CYCLES data and standard synoptic information, including buoy reports, and the GOES-West imagery. Notice how the front lies along the leading edge of the water vapor gradient, which is in good agreement with the findings from Seasat SMMR data by Katsaros and McMurdie (1983); notice how the integrated water vapor appears to define the frontal location more precisely than other available information. The integrated liquid water patterns (Fig. 4), in spite of the odd looking negative numbers, show contours nicely aligned with the edge of both the cloud band and the front.

Figure 5 is a plot of the SMMR rain rates (30 km resolution). The undulated 1 mm/hr rain rate contour duplicates almost exactly the detailed frontal analysis (see insert) of Hobbs and Persson (1982) based on doppler radar data and valid at 0100 PST. Evidently SMMR reveals the same meso-scale features occurring along the cold front as seen by the sophisticated radar.

We find, however, that the SMMR rain rates are generally lower than rain gauge values by a factor of 3 to 4, if we advect raining air parcels unchanged towards the coast with velocities estimated from synoptic wind fields and the frontal motion (cf. table in Gloersen *et al.*, 1984). Although most of the precipitation occurs as widespread rain in these midlatitude cyclones, some of the discrepancy may be due to insufficient resolution of SMMR. However, possible effects of the topography on the rain gauge values make it difficult to draw definite conclusions about the seriousness of this limitation (for further discussion see Katsaros and Lewis, 1984). The time of the onset of coastal precipitation appears to be predictable 12 to 24 hours in advance with good accuracy (within two to three hours) by this advection technique found from this and several other case studies. In other case studies we have examined (all during February and March, 1979), SMMR



Fig. 2. Infra-red imagery from the GOES-West satellite valid at 0045 PST 27 February, 1979. The dark solid line depicts the position of the cold front at 0100 PST as determined from buoy data, results from Hobbs and Persson (1982), and from the IR imagery itself.

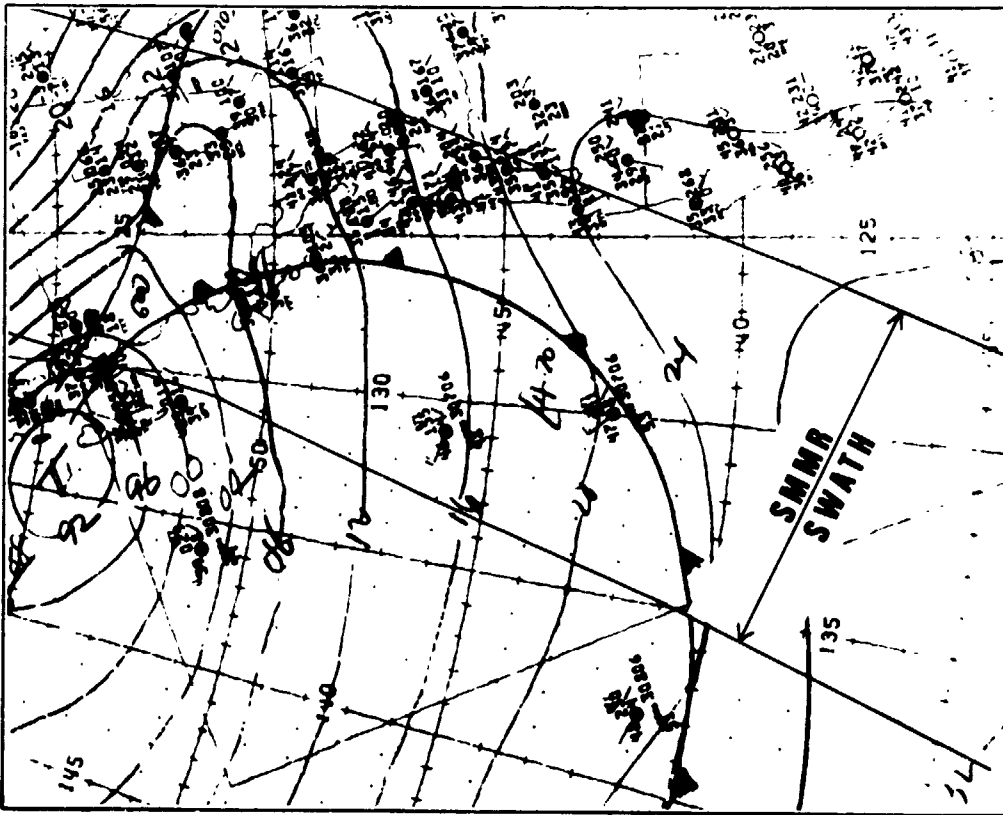


Fig. 1. The National Weather Service surface weather map analysis valid at 0100 Pacific Standard Time (PST) 27 February, 1979. The boundary of the SMMR swath is superimposed.

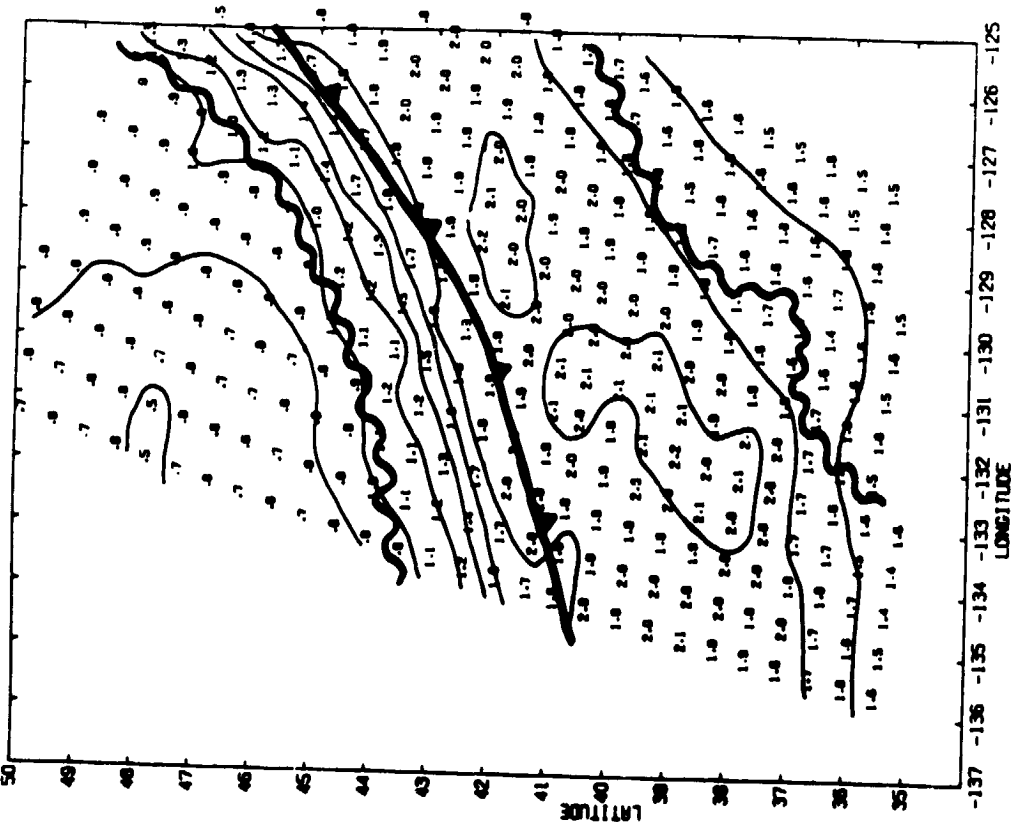


Fig. 3. SMR values of integrated water vapor ( $\text{gm}/\text{cm}^2$ ). The thin lines are contours at intervals of 0.2. The thick wavy lines depict the northern and southern boundaries of the frontal cloud band revealed by IR imagery (Fig. 1). Also shown is the location of the cold front as determined from independent data.

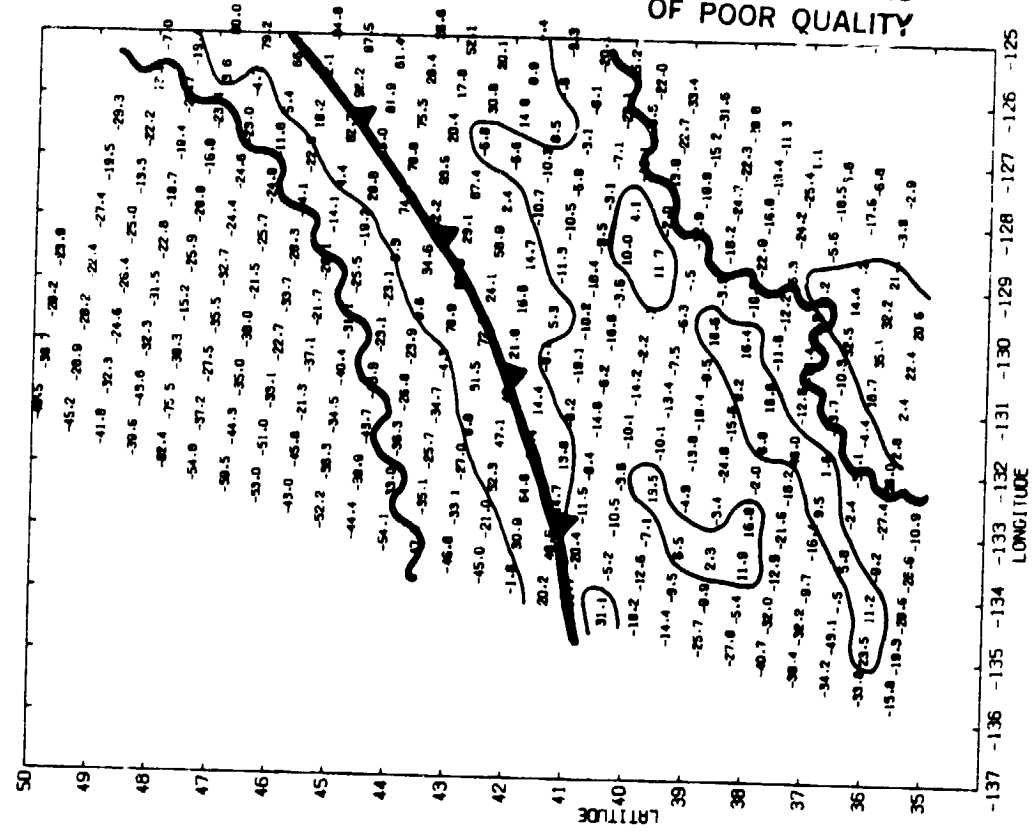
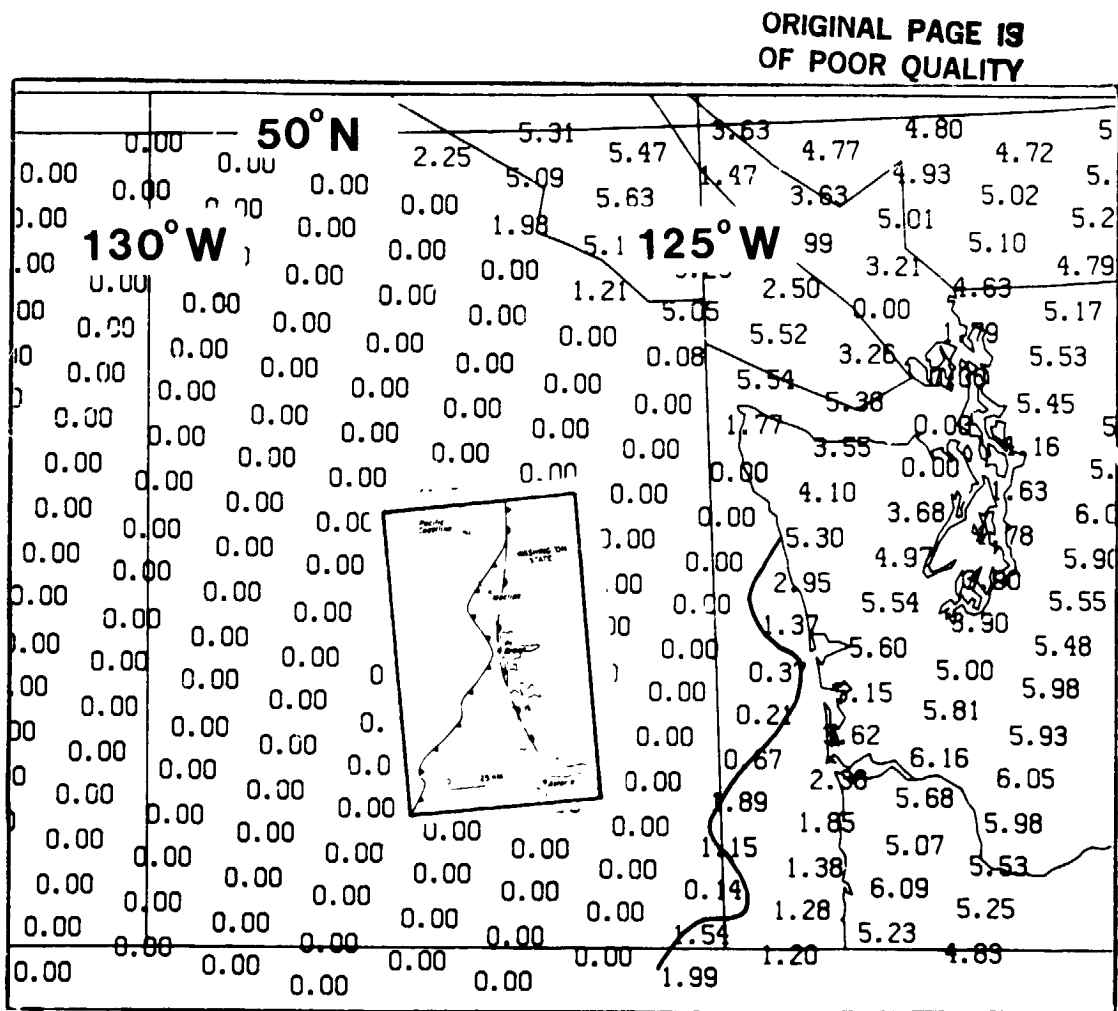


Fig. 4. SMR pattern of total cloud liquid water content. Units are  $10^{-4} \text{ gm}/\text{cm}^2$  but an unknown problem which is thought to cause a constant bias effect has resulted in some negative numbers. The thin solid lines denote the zero contour. All else as in Fig. 3.

rain rates are found to be in much better agreement with observed coastal rainrates, being of the same general magnitude (cf. Katsaros and Lewis, 1984).



**Fig. 5.** SMMR rainrates from part of orbit 1743 (mm/h). Half of the data is plotted (only half of the columns but all of the rows). The 1 mm/h contour has been drawn using all of the data. And shown both oriented and to scale is a reproduction of Fig. 9 of Hobbs and Persson (1982) depicting their analysis of the surface frontal location near the coast.

**3.2 Case Study B: Portion of Orbit 1992 Off the Coast of the Pacific Northwest, Centered at 0119 PST, 17 March, 1979**

This swath of Nimbus 7 SMMR data crossed a weak occluded frontal system on a southbound pass. The frontal location, determined without the use of SMMR

information, coincides closely with the back edge of the cloud band on the GOES-West image (Fig. 6) and has been superimposed on the SMMR integrated water vapor map (Fig. 7).

Again we see that the cold front coincides with the leading edge of the strong gradient in integrated water vapor. In addition, notice the interesting structure observed by SMMR ahead of the front. For example, the tongue of dry air diagnosed immediately east of the front appears to correspond to a break in the cloud band which exposed the ocean surface to the "view" of the GOES-West satellite (the  $1.8 \text{ gm/cm}^2$  contour has been superimposed on the infrared image in Fig. 6).

The liquid water content pattern (not shown) places highest values along and just ahead of the cold front. SMMR diagnoses a double band of high liquid water content showing some similarity to the double-banded nature of the clouds south of  $42^\circ\text{N}$  (see Fig. 6).

The SMMR rainfall pattern (also not shown) diagnoses a region of rain occurring north of  $44^\circ\text{N}$ , with its eastern edge located coincidentally with the surface front and extending eastward by as much as 200 km.

#### 4. CONCLUDING REMARKS

The new type of data provided by passive microwave sensing of the atmosphere over the sea provides us with the challenge of fully learning to understand what these signals mean and with the opportunity to put the data in the contexts of both operational and research work.

##### 4.1 Summary of Findings

In spite of the limited background knowledge for development of the SMMR algorithms for atmospheric integrated water vapor, liquid water and rain rate, for the "old" mid-latitude cyclones we have studied, these parameters look very convincing. Even if we must think of some of this information as qualitative at this stage, it is at least as useful as the familiar satellite imagery in locating surface fronts over the sea. We can identify liquid water regions within cloud systems, and they are in expected regions when compared to cloud imagery and location of fronts. The rainfall data can also identify frontal locations. They show meso-scale features of rainfall distribution in agreement with present knowledge about such structures, and the amounts given by the very simple algorithms are of the same magnitude as the areal rainfall average for most of our case studies.

##### 4.2 Gaps in Our Knowledge or Understanding

We have several kinds of gaps in our knowledge related to SMMR measurements and the water in the atmosphere as vapor, cloud droplets or raindrops:

First, we have incomplete information about how these parameters vary on the meso-scale, and, in particular, how they vary in storms at different stages of their development and in different regions of the ocean. This information is potentially obtainable from passive microwave measurements, but without some knowledge of the variability from other work, we cannot estimate what errors we might incur with limited spatial resolution.

Second, we don't know how accurately passive microwave instruments can determine liquid water content and rainfall rate, since we have not yet verified

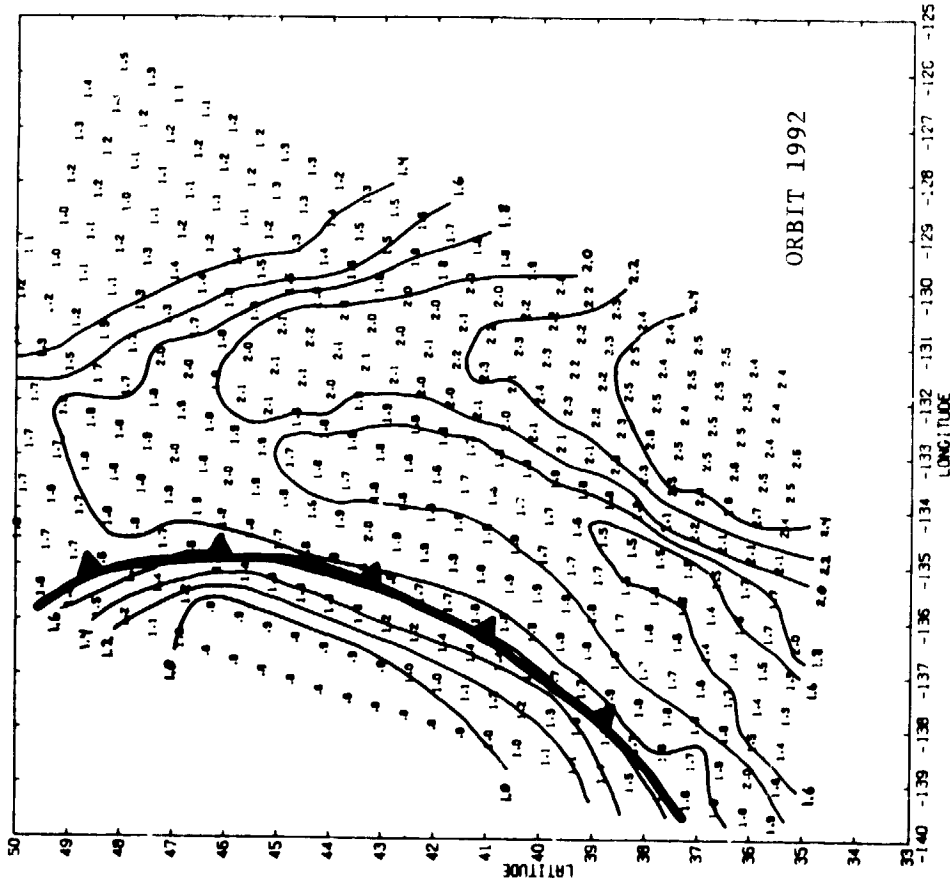


Fig. 7. SMMR values of integrated water vapor ( $\text{gm}/\text{cm}^2$ ) obtained at 0116 PST 17 March, 1979. Contours are drawn at  $0.2 \text{ gm}/\text{cm}^2$  intervals. The independently determined cold frontal location is superimposed.



Fig. 6. GOES-West enhanced IR imagery valid at 0215 PST 17 March, 1979. The equivalent blackbody temperature scale is defined at the top in intervals of  $10^\circ\text{C}$ . Superimposed is the  $1.8 \text{ gm}/\text{cm}^2$  water vapor contour (from Fig. 7).

the algorithms on the relevant spatial scales. Theoretical studies by Wilhelm et al. (1977) show dependencies on assumed droplet distribution and freezing level. How variable are these parameters? Can they be accounted for by adding another measurable quantity to the algorithms?

Third, we don't know how to use some of this new information. If real time integrated water vapor maps consistently tell us where the fronts are, an operational meteorologist would certainly know how to use that information, but how do we use integrated cloud liquid water and rainfall data? Can we relate these measures to the energetics or development of a storm (particularly its future)? If we only have occasional sampling from polar orbiting satellites, how do we make use of the information operationally or statistically for climatology?

It is known that total cloud liquid water content can be used to parameterize the absorption of visible light by the cloud and it is also a measure of emissivity of infrared radiation (e.g. DeVault and Katsaros, 1982). Could we use these relationships to calculate the radiative heat budget at the sea surface?

Other possible uses for this type of data is in estimating the role of water phase chemistry in the atmosphere and to estimate precipitation efficiency from the relative values for cloud liquid water and rainfall rate (Dean Hegg, 1984, personal communication). Can microwave data be obtained accurately enough for such interpretations?

Integrated water vapor in conjunction with sea surface temperature and winds have been used to estimate the evaporation rate from the sea (W. T. Liu, personal communication). What is the ultimate accuracy of such parameterizations?

#### 4.3 Recommendations for Further Work and Experiments

We need direct comparisons between passive microwave observations of storm systems and in situ areally averaged measurements of the relevant parameters. This would require dedicated experiments designed specifically for this purpose (at least some dedicated resources) using two or more instrumented aircraft and perhaps upward looking radiometers on small islands or ships.

We also need to pursue theoretical and experimental work on finding the optimum microwave frequencies or combination of frequencies for measuring the various atmospheric water parameters.

And, now that these new measures are within reach, we need simulation type experiments to find imaginative ways to include them in the diagnosis and prognosis of atmospheric storms.

#### 5. REFERENCES

Alishouse, J. C., 1983: Total precipitable water and rainfall determinations from the Seasat Scanning Multichannel Microwave Radiometer (SMMR). *J. Geophys. Res.*, 88, 1929-1935.

DeVault, J. E. and K. B. Katsaros, 1982: Remote Determination of Cloud Liquid Water Path from Bandwidth-Limited Shortwave Measurements. Contribution No. 646, Dept. of Atmospheric Sciences, University of Washington, Seattle, WA.

Gloersen, P., D. J. Cavalieri, A. T. C. Chang, T. T. Wilhelm, W. J. Campbell, O. M. Johannessen, K. F. Kunzi, D. B. Ross, D. Staelin, E. P. L. Windsor, F. T. Barath, P. Gudrandsen, E. Langham, R. O. Ramseier and K. B. Katsaros, 1983: A summary of results from the first Nimbus 7 SMMR observations. *J. Geophys. Res.* (submitted).

Hobbs, P. V. and P. O. G. Persson, 1982: The mesoscale and microscale structure and organization of clouds and precipitation in midlatitude cyclones. Part V: The substructure of narrow cold-frontal rainbands. *J. Atmos. Sci.*, 39, 280-295.

Katsaros, K. B. and K. M. Lewis, 1984: Studies of Atmospheric Water Parameters in North Pacific Cyclones with the Nimbus 7 Scanning Multichannel Microwave Radiometer. Technical Report, Contracts NAS 5-26262, NAG 5-354. Dept. of Atmospheric Sciences, University of Washington, Seattle, WA (in preparation).

Katsaros, K. B. and L. A. McMurdie, 1983: Atmospheric water distribution in cyclones as seen with Scanning Multichannel Microwave Radiometers (SMMR). Presentation made at IGARSS'83, San Francisco, CA, 31 August-2 September, 1983.

Katsaros, K. B., P. K. Taylor, J. C. Alishouse and R. J. Lipes, 1981: Quality of Seasat SMMR (Scanning Multichannel Microwave Radiometer) atmospheric water determinations. *Oceanography from Space*, 691-706, Plenum Publishing Corp., New York.

McMurdie, L. A., 1983: Seasat Passive Microwave Observations of North Pacific Cyclones. M.S. Thesis, Dept. of Atmospheric Sciences, University of Washington, Seattle, WA.

Nimbus 7 Scanning Multichannel Microwave Radiometer, User's Guide, 1984 (in preparation).

Njoku, E. G., E. J. Christensen and R. E. Cofield, 1980: The Seasat Scanning Multichannel Microwave Radiometer (SMMR) antenna pattern correction development and implementation. *IEEE J. Oceanic Eng.*, OE-5, No. 2, 125-137.

Persson, P. O. G., 1980: The Small Mesoscale Structure and Microphysics of a Narrow Cold-Frontal Rain Band. M.S. Thesis, Dept. of Atmospheric Sciences, University of Washington, Seattle, WA.

Taylor, P. K., T. H. Guymer, K. B. Katsaros and R. G. Lipes, 1983: Atmospheric water distributions determined by the Seasat Multichannel Microwave Radiometer. Variations in the Global Water Budget, 93-106, A. Street-Perrott et al., eds. D. Reidel Publishing Company, Dordrecht, Holland.

Wilheit, T. T. and A. T. C. Chang, 1980: An algorithm for retrieval of ocean surface and atmospheric parameters from the observations of the Scanning Multichannel Microwave Radiometer (SMMR). *Radio Science*, 15, 525-544.

Wilheit, T. T., A. T. C. Chang, M. S. V. Rao, E. B. Rodgers and J. S. Theon, 1977: A satellite technique for quantitative mapping rainfall rates over the ocean. *J. Appl. Meteor.*, 16, 551-560.

## 6. ACKNOWLEDGEMENTS

This work was performed under NASA Grant NAG 5-354. We appreciate the valuable advice from Prof. Richard J. Reed on the frontal analysis and the assistance rendered with the typing of this manuscript by Ms. Sylvia Lavin. Contribution No. 696, Department of Atmospheric Sciences, University of Washington Seattle, WA, U.S.A.